

# Role of Graphene Oxide in Disentangling Amyloid Beta Fibrils

Brianna Duswalt <sup>1</sup>, Isabella Wolson <sup>2</sup> and Isaac Macwan <sup>1,\*</sup>

<sup>1</sup> Department of Electrical and Biomedical Engineering, Fairfield University, Fairfield, CT 06824, USA; brianna.duswalt@student.fairfield.edu

<sup>2</sup> Davidson School of Chemical Engineering, Purdue University, West Lafayette, IN 47907, USA; iwolson@purdue.edu

\* Correspondence: imacwan@fairfield.edu; Tel.: +1-203-254-4000

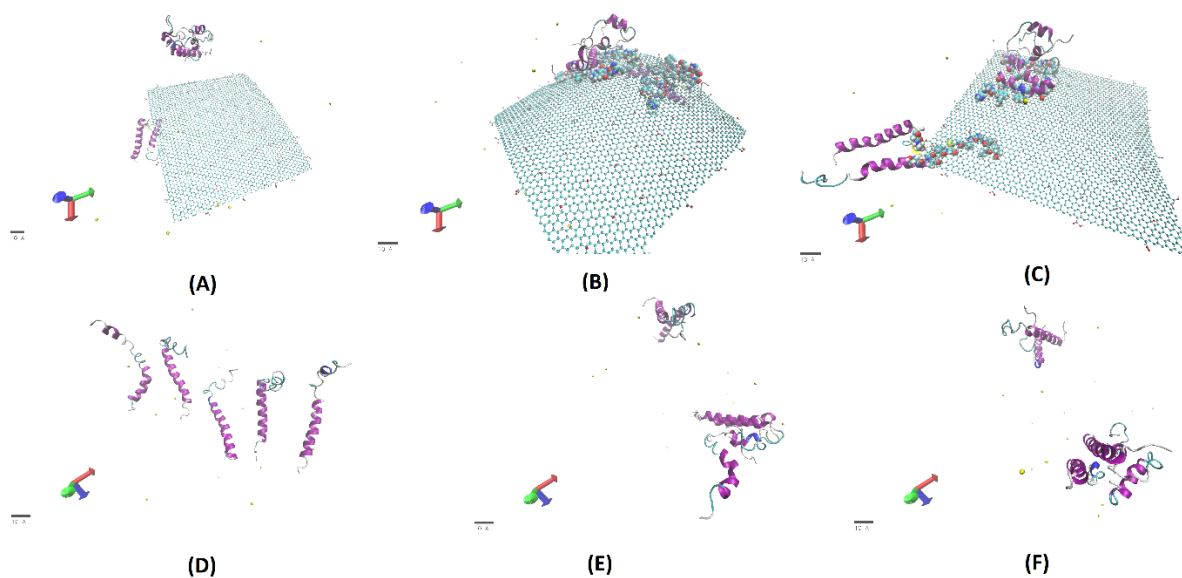


Figure S1. Trajectory screenshots for the 100-ns molecular simulations of the individual A $\beta$  monomers: (A) 5 A $\beta$  monomers after minimization and equilibration at 0 ns; (B) 5 A $\beta$  monomers over the surface of graphene oxide (GO) at 50 ns; (C) 5 A $\beta$  monomers over the surface of GO at 100 ns; (D) The 5 A $\beta$  monomers in a control simulation in the absence of GO at 0 ns; (E) 5 A $\beta$  monomers in the control simulation in the absence of GO at 50 ns; (F) 5 A $\beta$  monomers in the control simulation in the absence of GO at the end of 100 ns simulation run. The A $\beta$  monomers are represented with the New Cartoon representation in VMD, whereas GO and the sodium ions are represented with the CPK (Corey-Pauling-Koltun) model. Water molecules are not shown for clarity.

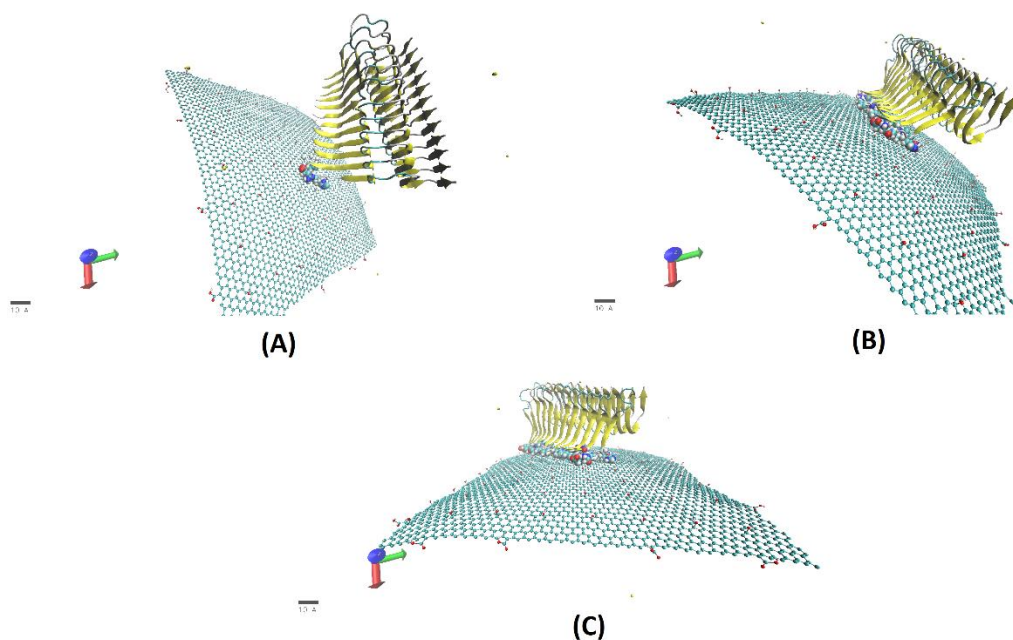


Figure S2. Trajectory screenshots for the 200 ns molecular simulation of the A $\beta$  fibril in the presence of GO: (A) A $\beta$  fibril on the verge of interacting with the GO surface after the minimization and equilibration runs and starting at 0 ns of the production run; (B) A $\beta$  fibril adsorbed on the surface of GO at 100ns in the simulation; (C) A $\beta$  fibril firmly adsorbed on the surface of GO at the end of the simulation run at 200 ns. The A $\beta$  fibril is represented with the New Cartoon representation in VMD, whereas GO and the sodium ions are represented with the CPK (Corey-Pauling-Koltun) model. Water molecules are not shown for clarity.

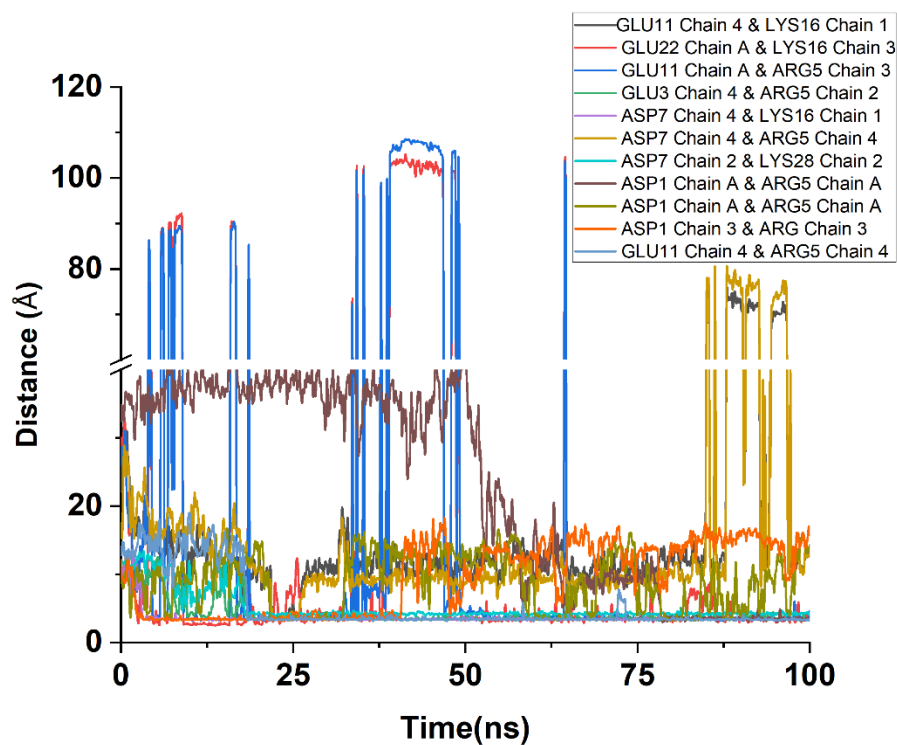


Figure S3: Plots showing individual salt bridges for the 5-A $\beta$  system in the absence of GO (control simulation).

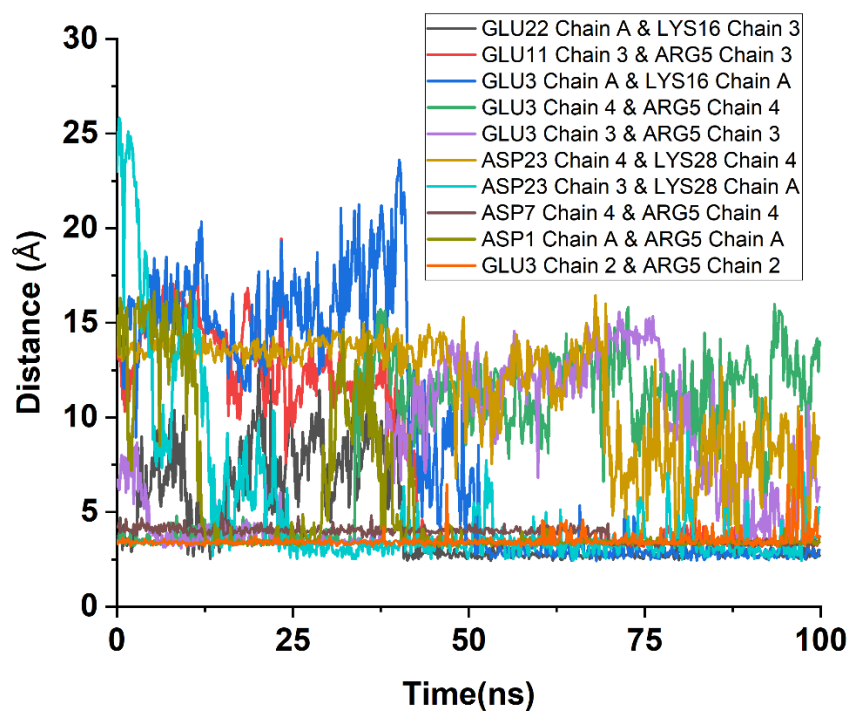


Figure S4: Plots showing individual salt bridges for the 5-A $\beta$  system in the presence of GO.

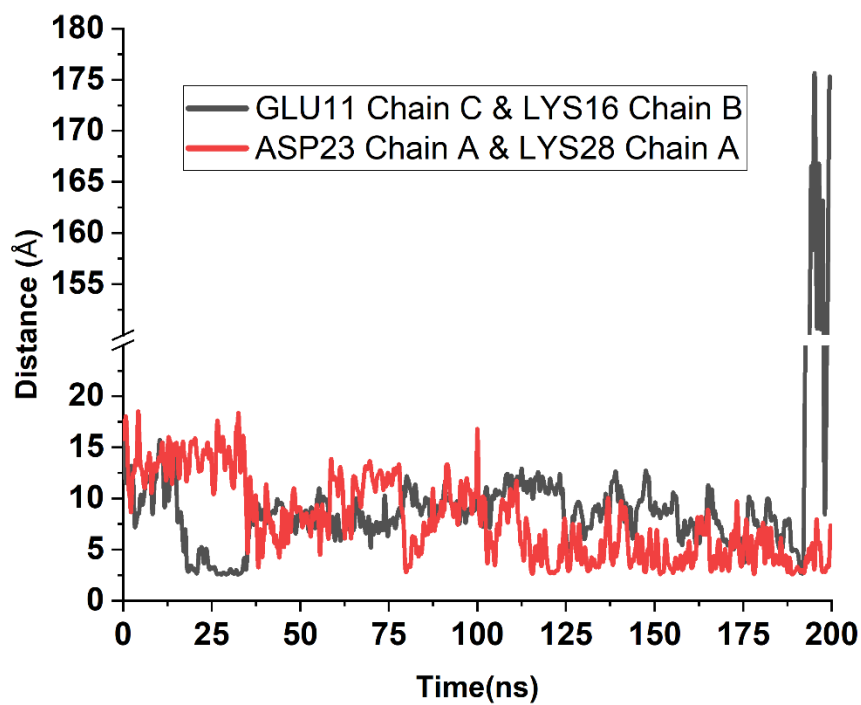


Figure S5: Plots showing individual salt bridges for the 12-A $\beta$  fibril system in the presence of GO.

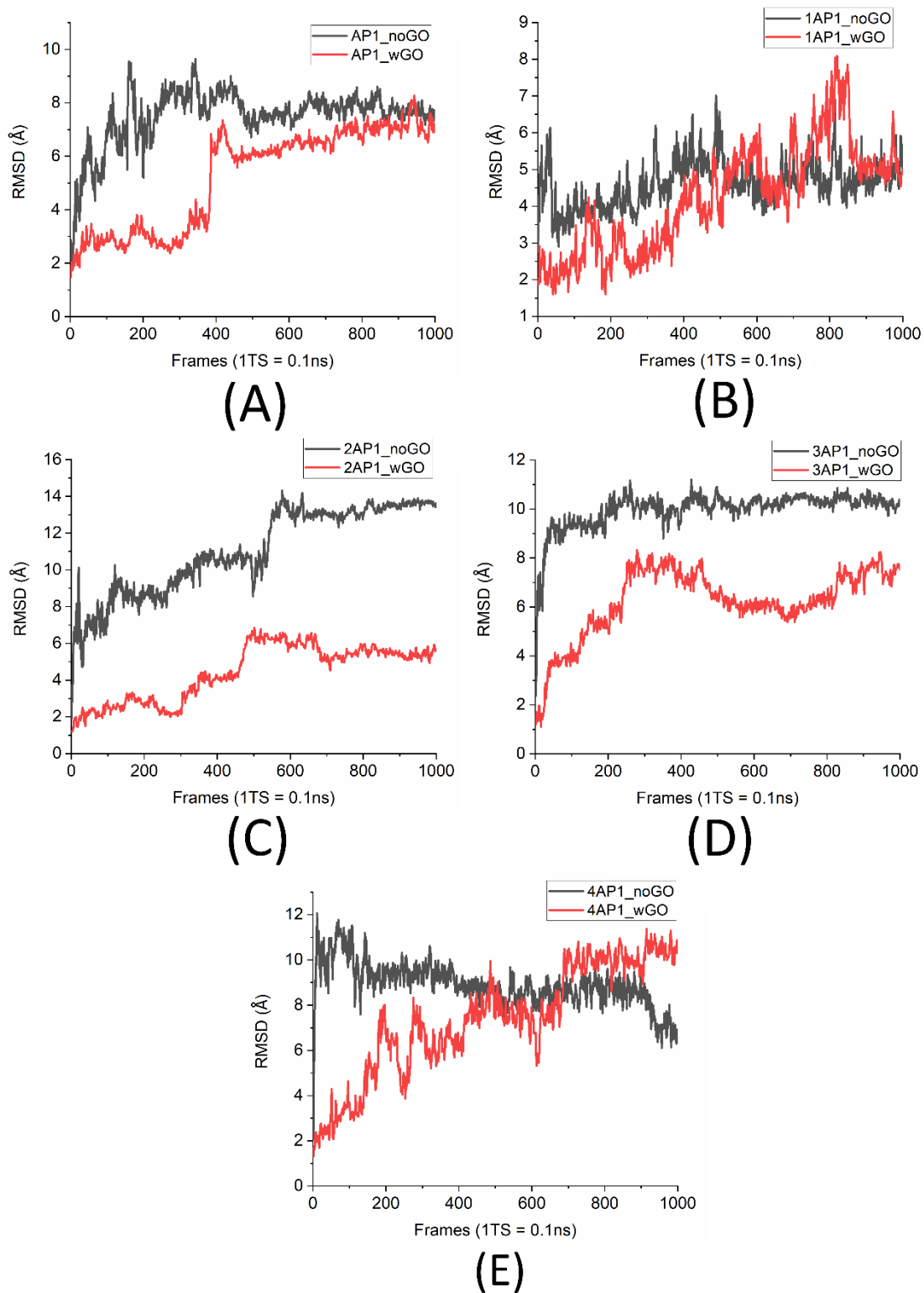


Figure S6. Root Mean Square Deviation (RMSD) of individual Aβ monomers within the 5-Aβ system, in the presence and absence of GO: (A) Monomer segment AP1; (B) Monomer segment 1AP1; (C) Monomer segment 2AP1; (D) Monomer segment 3AP1; (E) Monomer segment 4AP1.

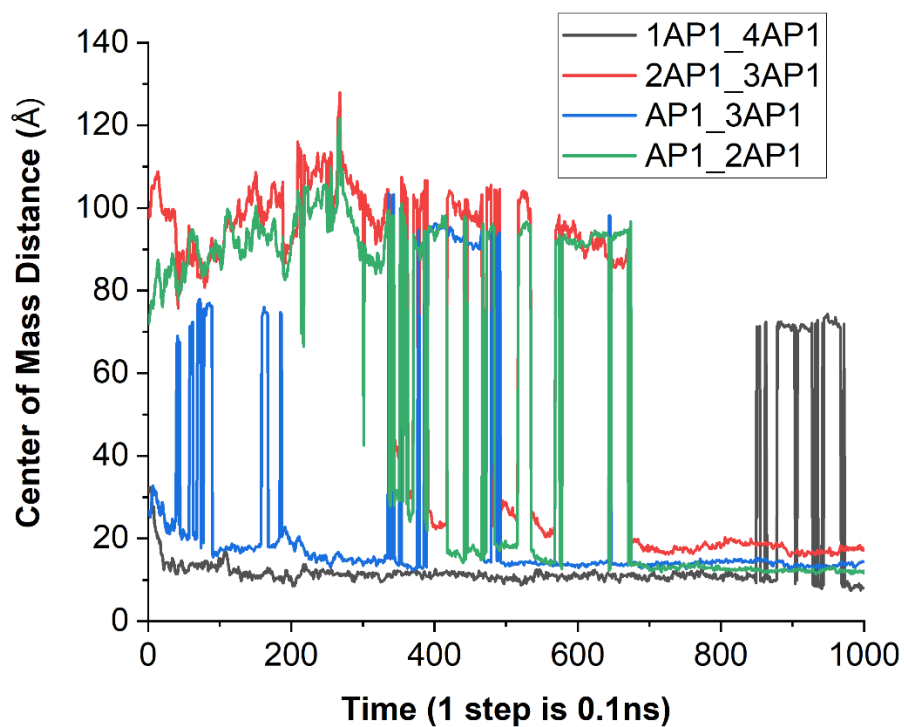


Figure S7: Plots showing distance between the center of mass of the individual monomers within the the two clumps (clump 1 involving the segments AP1, 2AP1 and 3AP1, and clump 2 involving the two segments 1AP1 and 4AP1) in the absence of GO.

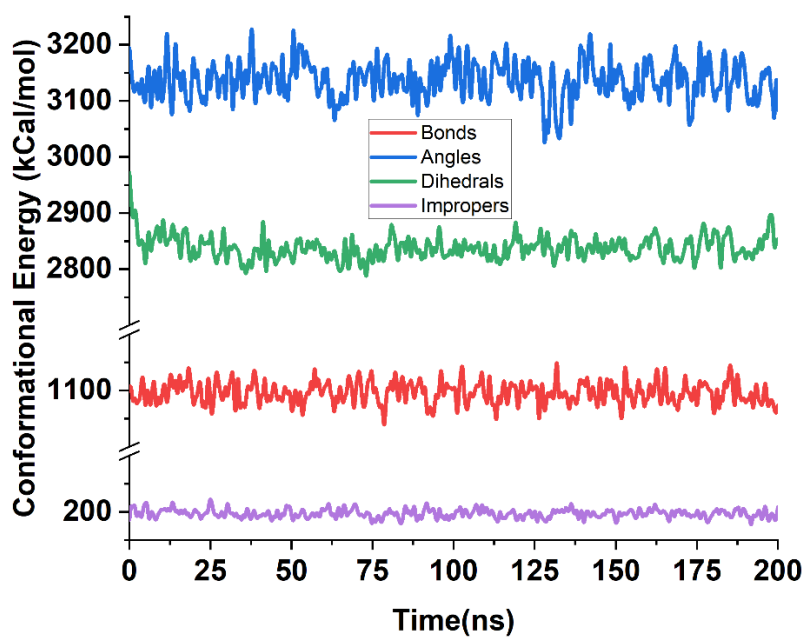


Figure S8: Conformational energy plots showing individual structural energies for the 12-A $\beta$  fibril system in the presence of GO.

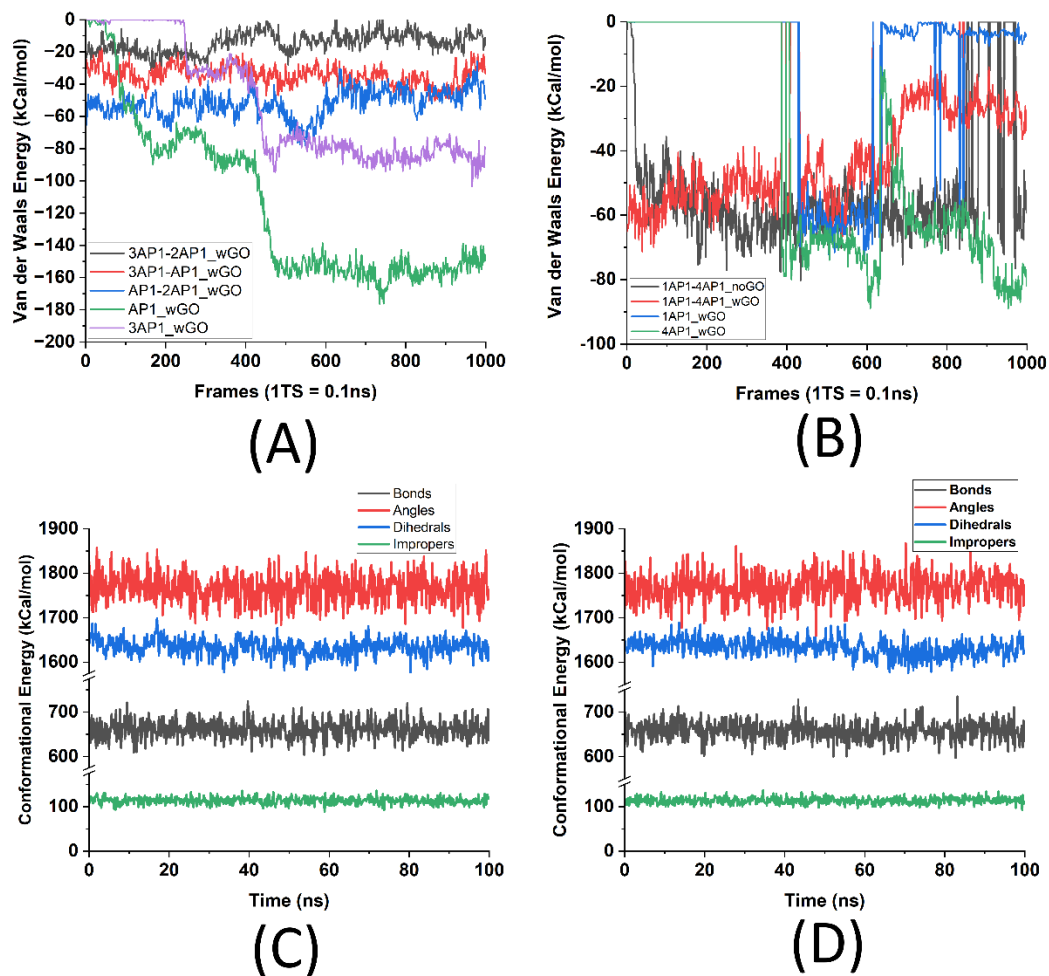


Figure S9. Interaction and conformational energies between and within the individual  $A\beta$  monomers of the 5- $A\beta$  system: (A) Interaction energy in the form of Van der Waals between the individual monomers within clump 1 and that between the monomers and GO; (B) Interaction energy in the form of Van der Waals between the individual monomers within clump 2 and that between the monomers and GO; (C) Conformational energies of the bonds, angles, dihedrals and impropers of the individual monomers within the 5- $A\beta$  system in the presence of GO; (D) Conformational energies of the bonds, angles, dihedrals and impropers of the individual monomers within the 5- $A\beta$  system in the absence of GO.

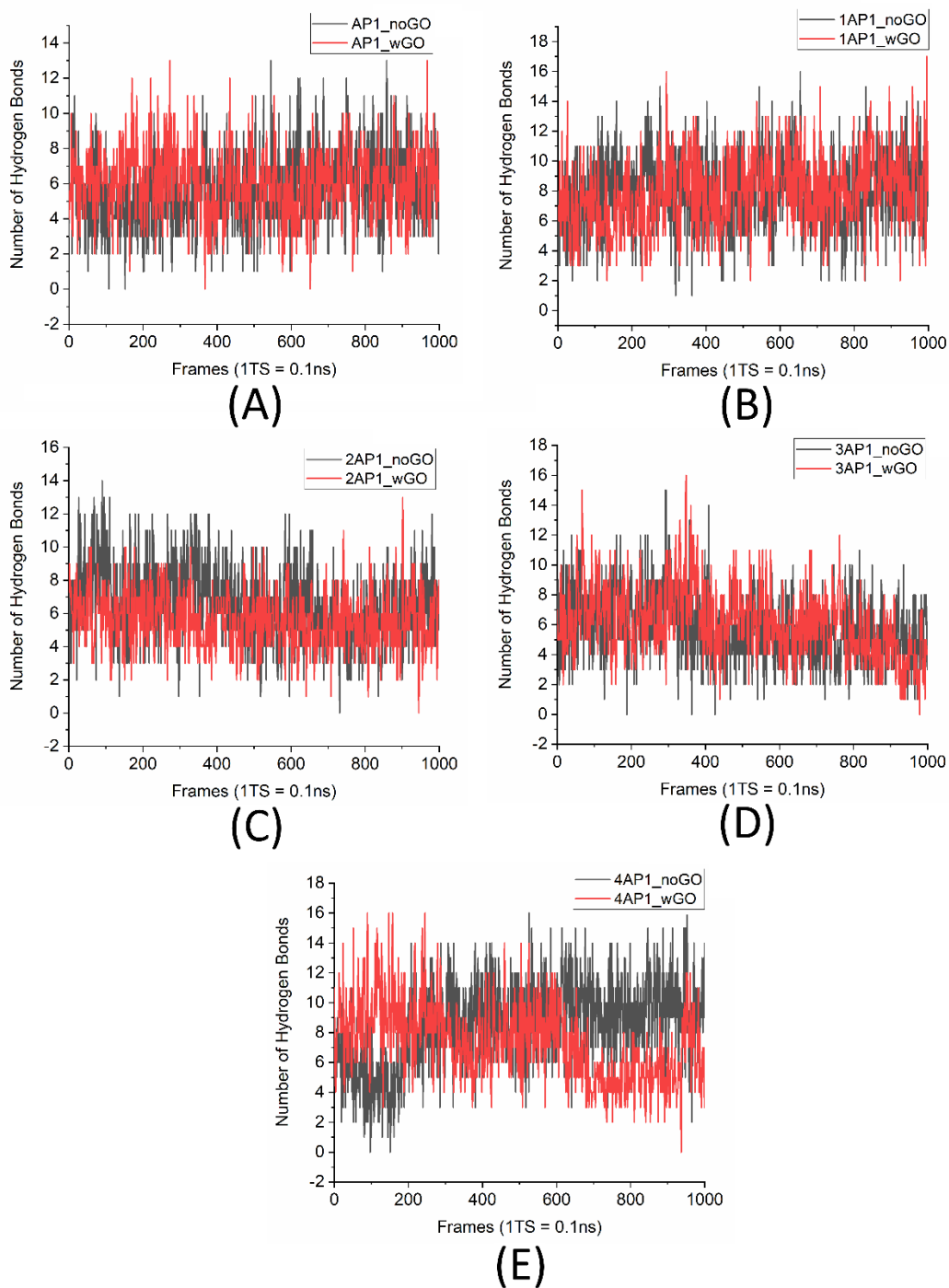


Figure S10. Comparison of the number of hydrogen bonds within the individual A $\beta$  monomers of the 5-A $\beta$  system in the presence and absence of GO: (A) Number of hydrogen bonds within the segment AP1 in the presence and absence of GO; (B) Number of hydrogen bonds within the segment 1AP1 in the presence and absence of GO; (C) Number of hydrogen bonds within the segment 2AP1 in the presence and absence of GO; (D) Number of hydrogen bonds within the segment 3AP1 in the presence and absence of GO; (E) Number of hydrogen bonds within the segment 4AP1 in the presence and absence of GO.

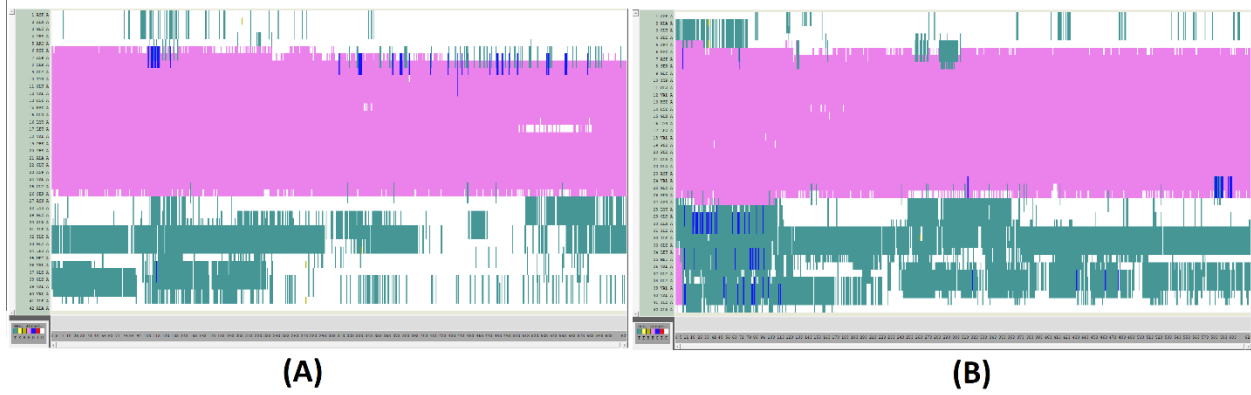


Figure S11: Secondary structure analysis of the segment AP1 in the presence (A) and absence (B) of GO.

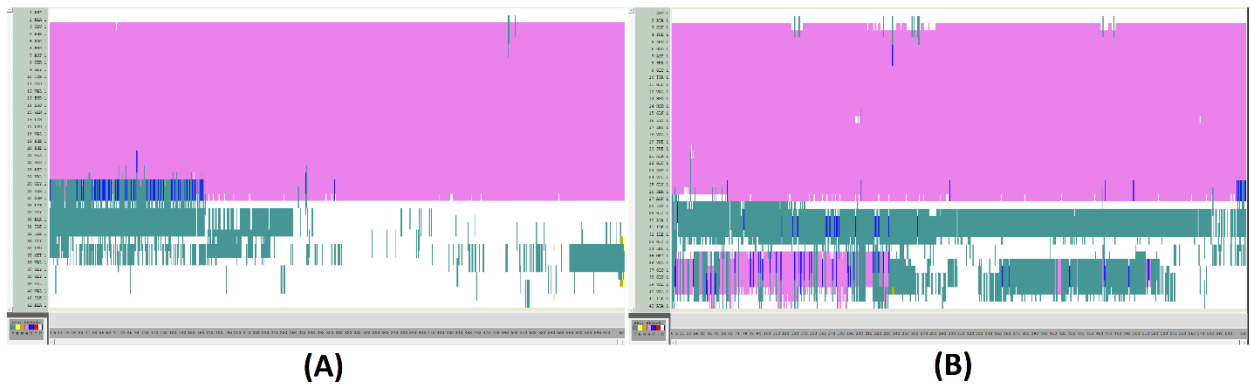


Figure S12: Secondary structure analysis of the segment 1AP1 in the presence (A) and absence (B) of GO.

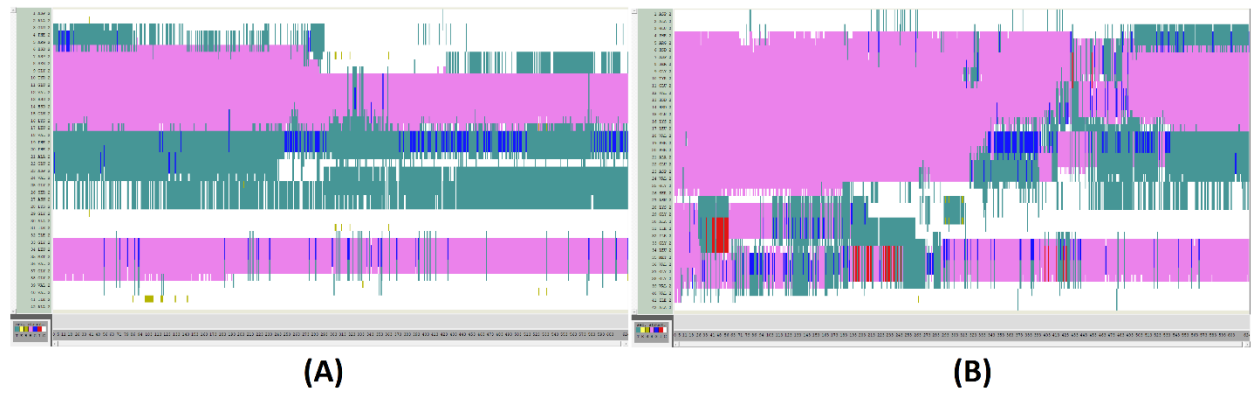


Figure S13: Secondary structure analysis of the segment 2AP1 in the presence (A) and absence (B) of GO.

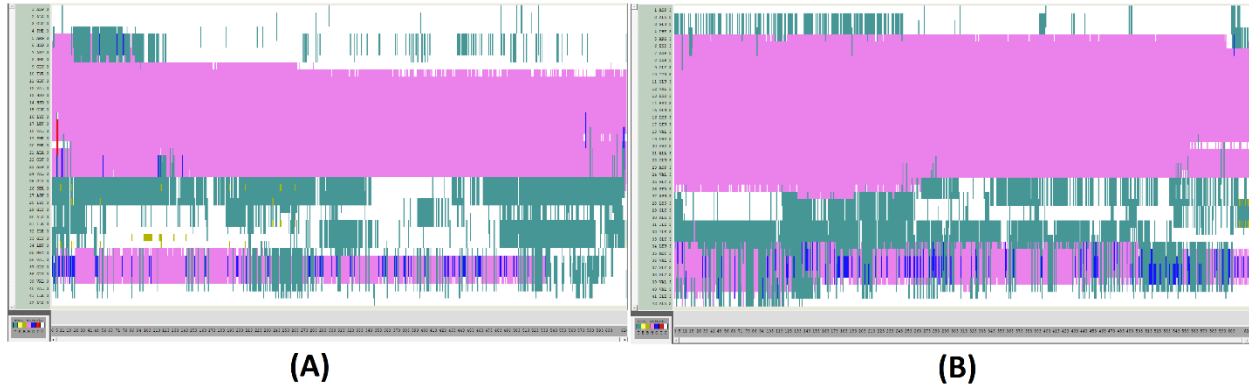


Figure S14: Secondary structure analysis of the segment 3AP1 in the presence (A) and absence (B) of GO.

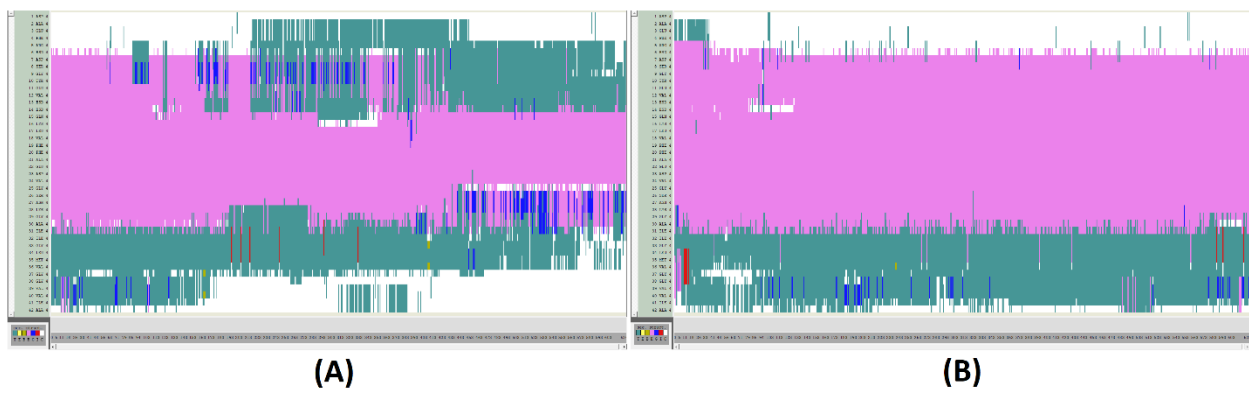


Figure S15: Secondary structure analysis of the segment 4AP1 in the presence (A) and absence (B) of GO.

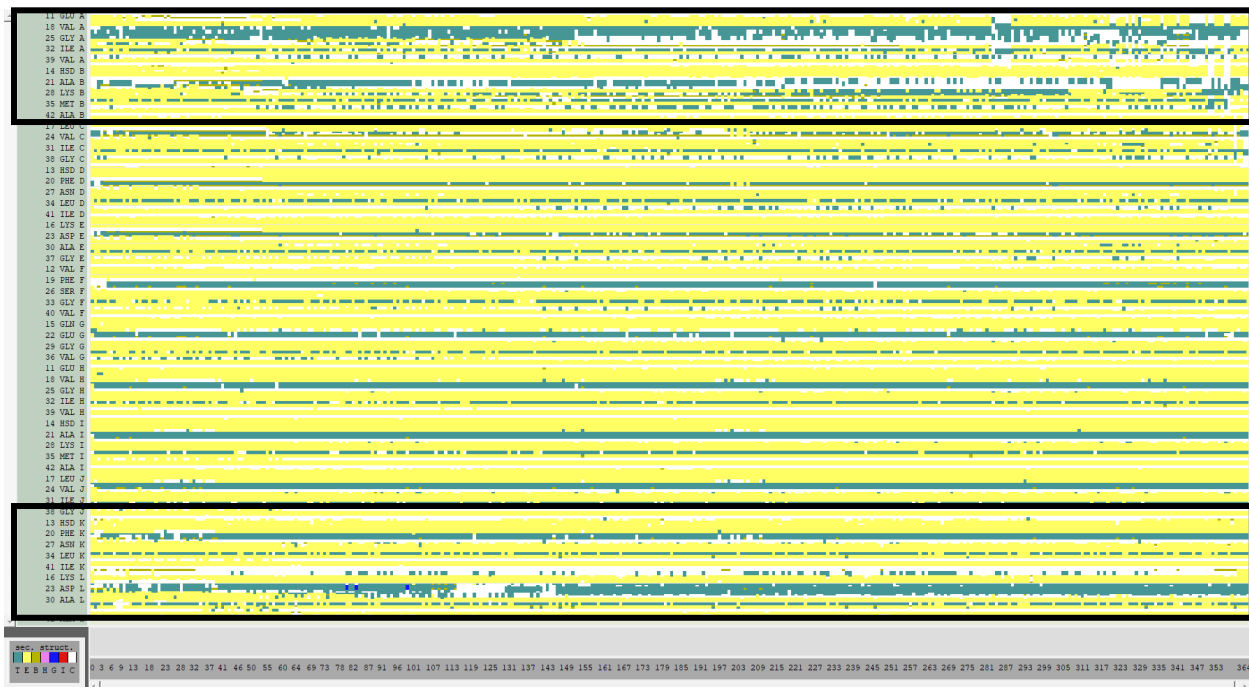


Figure S16: Secondary structure analysis of the 12-monomer fibril.

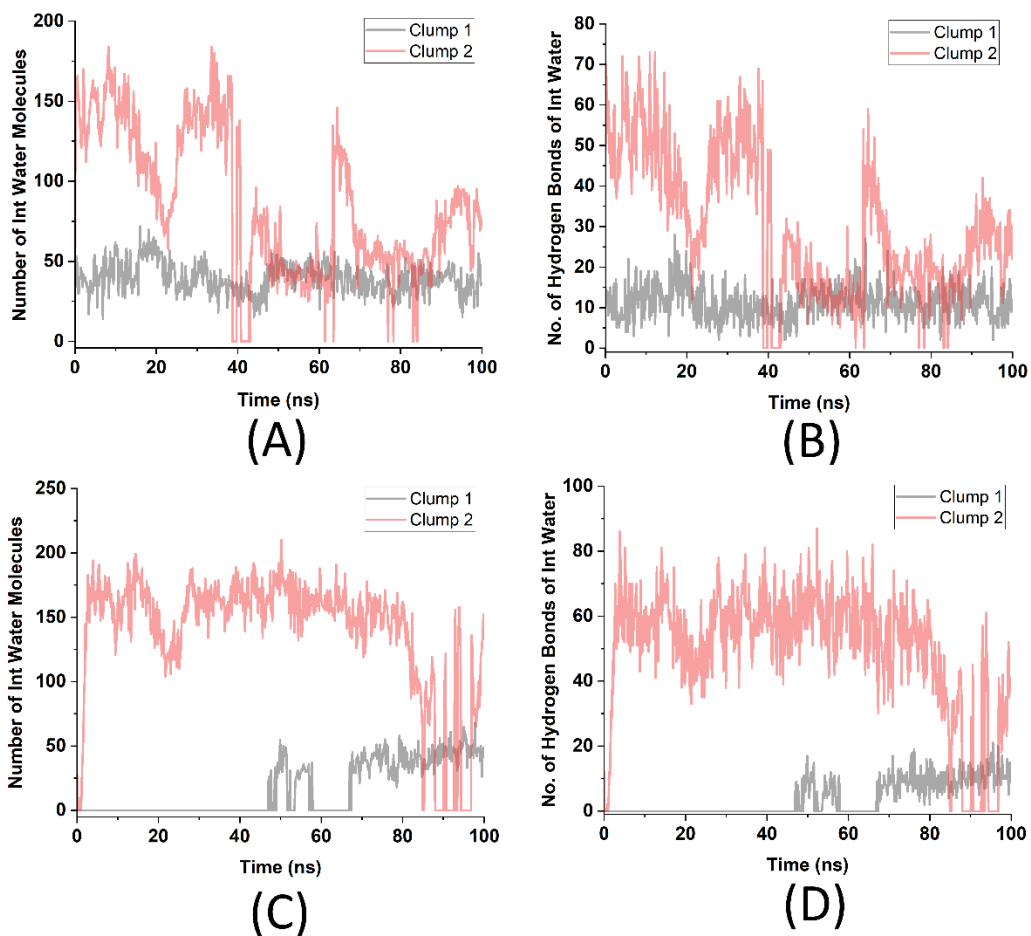


Figure S17. Quantification of the number of interfacial water molecules and their hydrogen bonds within the two clumps: (A) Number of interfacial water molecules between the segments AP1, 2AP1 and 3AP1 of clump 1, and segments 1AP1 and 4AP1 of clump 2 in the presence of GO; (B) Number of hydrogen bonds of the interfacial water molecules between the segments AP1, 2AP1 and 3AP1 of clump 1, and segments 1AP1 and 4AP1 of clump 2 in the presence of GO; (C) Number of interfacial water molecules between the segments AP1, 2AP1 and 3AP1 of clump 1, and segments 1AP1 and 4AP1 of clump 2 in the absence of GO; (D) Number of hydrogen bonds of the interfacial water molecules between the segments AP1, 2AP1 and 3AP1 of clump 1, and segments 1AP1 and 4AP1 of clump 2 in the absence of GO.

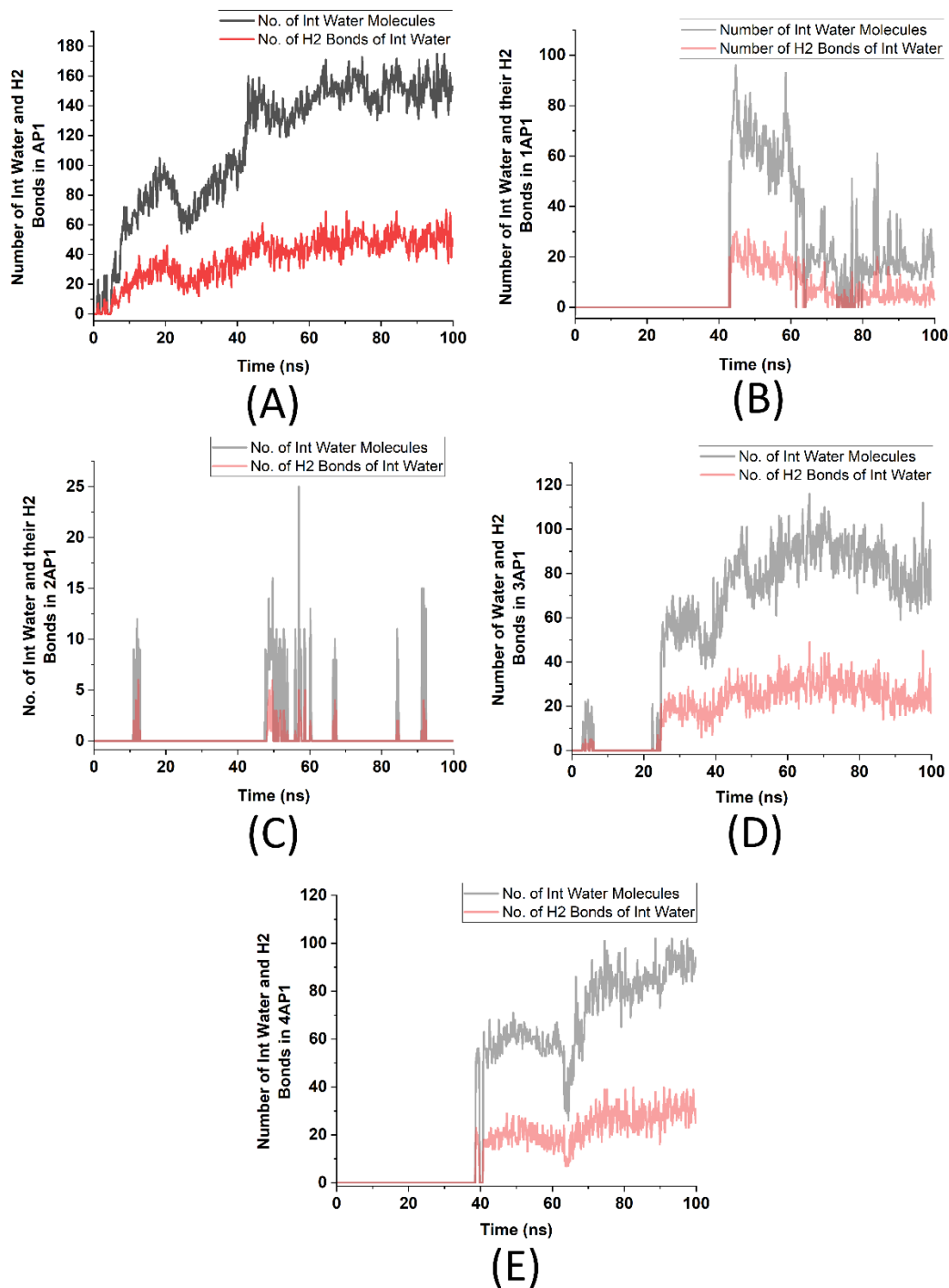


Figure S18. Quantification of the number of interfacial water molecules and their hydrogen bonds between the individual A $\beta$  monomers and GO: (A) Number of interfacial water molecules and their respective hydrogen bonds between segment AP1 and GO; (B) Number of interfacial water molecules and their respective hydrogen bonds between segment 1AP1 and GO; (C) Number of interfacial water molecules and their respective hydrogen bonds between segment 2AP1 and GO; (D) Number of interfacial water molecules and their respective hydrogen bonds between segment 3AP1 and GO; (E) Number of interfacial water molecules and their respective hydrogen bonds between segment 4AP1 and GO.